IL NUOVO CIMENTO Vol. 37 C, N. 4 Luglio-Agosto 2014
DOI 10.1393/ncc/i2014-11796-0

Communications: SIF Congress 2013

The planetesimal-driven migration of planets: Observational consequences

F. Panichi(*)

Dipartimento di Fisica e Astronomia - viale Berti Pichat 6/2 - 40127 Bologna, Italy

ricevuto il 31 Gennaio 2014; approvato il 9 Maggio 2014

Summary. — The role of planetary migration in a non–self-gravity planetesimals disk is analyzed in this paper. I calculate the migration rate exerted on a planet due to the gravitational interaction with a planetesimals disk both numerically and analytically. I use two different configurations for the disk-planet interaction: co-rotating (with an inclination of 0° with respect to the plane of motion of the disk) and counter-rotating (with an inclination of 180°) planet. I perform 2D numerical simulations of disks with 10^4 planetesimals with or without a Rayleigh distribution in eccentricity. I show that counter- and co-rotating planets have different migration rates: retrograde planets migrate faster than the prograde ones. The migration rate depends on the ratio between the planet to planetesimal mass and on the initial mean eccentricity of planetesimals. I compare numerical simulations with analytical theories of dynamical friction and linear theory of density waves. In both cases each theory can explain only parts of the simulation results. A more general and powerful analytical theory of planet migration must be realized. Finally I simulate the observation of co- and counter-rotating massless disks of planetesimals with the interferometer ALMA. With the high resolution of ALMA it is possible to characterize the gap created by the resonances overlap. I show that in the two cases different resonance conditions create gaps with different extensions which can be observed with ALMA for a distance of 100 parsec and a disk size of 100 A.U., and for disks of 20 A.U. and a distance of 50 parsec. With this simple method it is possible to calculate the planet's mass in both cases studying the indirect presence of the planet. The case of massive disks are also investigated. In this case planet migration creates a large modification of the planetesimals density profile that can be studied observing the brightness surface profile of the disk. Conversely to other detection methods, like radial velocity, this method is very powerful to discover planets very far from their host stars: the higher the distance of the planet from the star the greater the efficiency of this method.

PACS 96.30.-t – Solar system objects.
PACS 96.30.Bc – Comparative planetology.
PACS 96.12.-a – Planetology of solid surface planets.
PACS 96.12.Bc – Origin and evolution.

(*) E-mail: federico.panichi@studio.unibo.it

1. – Introduction

From the discovery of the first extrasolar planet [1] several exoplanets have been observed. A large variability in the orbital parameters has been detected [2]. In this paper I focus on the study of "hot planets": planets with a semimajor axis smaller than 1 A.U. Several theories and models have been proposed to explain the presence of planet so close to the host star. In this study I analyze the dynamical model based on the planetesimal-driven migration of a single planet [3-5]. This particular mechanism of migration is based on the angular-momentum exchange between planetesimal disk and large body and has been deeply investigated [6, 7].

Different theories predict the dependence of the migration rate (the variation of the semimajor axis of the planet in time) on the planet mass: migration independent of the planet mass [8], inversely proportional to the mass of the planet (*rapid migration* in [9]), directly proportional to the planet mass [10] or proportional to the cubic root of the planet mass [11]. Important progress is expected in the near future, from both the theoretical and observational point of view. In this preliminar and exploratory study, I focus on the expected observational features of circumstellar disks modified by the planetary migration in the co-rotating and counter-rotating cases. Surprisingly no research on the counter-rotating migration in a planetesimal or in a gas disks has been performed so far. With counter-rotating planet I define a planet which is inclined by 180° with respect to the orbital plane of planetesimals (and of the planet itself). Instead a considerable number of articles were written for counter-rotating migration of a binary black hole ([12] and references therein). This citation is important because some of the results in that article match with this work as, for instance, the more rapid migration of a "retrograde" planet with respect to a "prograde" one and the close encounter zone([1]) for this counter-rotating case is smaller with respect to the co-rotating planet due to the absence of resonances. At first, the counter-rotating disk may appear academic, however the very important Kozai mechanism [13] has been suggested as a possible origin for "retrograde" planets that may be 15% of all extrasolar objects ([14] and references therein). Also a small number of observations can suggest the presence of highly inclined exoplanet ([15] and references therein). Recent studies in the near infrared (NIR) have shown how most of the young stars possess a circumstellar disk [16]. The interaction between a planet and a disk can create different characteristic structures as *density spiral waves* [17] or *debris disks* [18]. The observation of these features can be done only with high-resolutions interferometer as, for example, ALMA (Atacama Large Millimeter Array) for both line emission [19] and direct imaging [20]. Important features can be observed and used to indirectly detect a planet embedded in this protostellar disk as, for example, a localized infrared excess due to resonant planetesimals [21] or the brightness profile asymmetry for the β-Pictoris disk [22]. Also in the late stage of planet formation, when all the gas has been dissipated and the planetesimals growth in size to kilometer dimensions, the interaction between these plantesimals re-create a dust disk with particular size (1–7 mm), that can radiate at particular wavelengths [23]. In sect. **2** I describe the numerical simulations, in sect. **3** I summarize the main results, while in sect. **4** I discuss the results and introduce the line of research I intend to pursue in forthcoming studies.

([1]) A highly interacting zone also called *scattering zone* or *feeding zone*.

2. – The simulations

I briefly describe the numerical simulations performed, and how the final density profiles of the modified disks are "observed" using ALMA mock observations.

2˙1. *Dead planet: modifications of the disk.* – In this first set of simulations the planet modifies the disk, but it is not affected by the disk itself. In practice, I am studying a large number of restricted three-body problems. Starting with the very simple circular, planar, restricted three-body problem I then relax the hypotesis of planetesimals in circular orbits to simulate an eccentric, planar, restricted three-body problem introducing a Rayleigh distribution for the plantesimals eccentricity e:

$$g(e) = 4\frac{\Sigma_{pl}}{m_{pl}}\frac{e}{\langle e^2\rangle}\exp\left[-\frac{e^2}{\langle e^2\rangle}\right], \tag{1}$$

in (1) the value $\langle e^2\rangle$ is the mean square value of the eccentricity of planetesimals, m_p their mass and Σ_{pl} the surface disk density. The mean square value of eccentricity (defined in (1)) spans from a minimum of 0 (circular obits) to a maximum of 10^{-4} (small eccentric orbits). For the massive disks a constant surface density (Σ_0) that scales linearly with the distance (r) of the planetesimals was introduced. The value of Σ_0, to keep the planet–to–planetesimal-mass ratio equal to 1/600th, varies everytime the planet mass varies. The constant surface density then spans from $1.3 \times 10^2\,\mathrm{gr\,cm^{-2}}$ for a planet with the mass of the Earth to $5 \times 10^3\,\mathrm{gr\,cm^{-2}}$ for a planet with the mass of Jupiter. These densities are very high due to the fact that I want to investigate the late stage of planet formation in which the planetesimals masses are very high [8, 24].

The simulations were done with the SWIFTER code [25] a N-Body numerical integration code. For this preliminar simulations I used the numerical integration routine RMVS [26], a very efficient integrator especially for close encounters. I kept the time step for each simulations equal to 1/20th of the orbital period of the innermost orbits (in general, 1 A.U.). The planet is in a circular orbit around the host star with a distance that varies from 5 to 30 A.U. in a planetesimal disk of radius from 20 to 60 A.U. with a inner hole of 10 A.U. for the smallest disk and of 20 A.U. for the largest one. I simulate disks with different dimensions to show how far is it possible observe the simulated disk with ALMA mock observations. Every simulations for both massless and massive disks run for 2×10^4 yr, with a planetesimals number equal to 10^4 for each disk's simulation and 4×10^3 for each ring simulation.

2˙2. *Live planet: backreaction and migration.* – With the experience obtained from the previous "dead" simulations I now proceed to investigate the back reaction of the disk on the planet. All the disks initial conditions are described in the previous section. In addition, I also performed some test simulation in which the planet interact with a ring of particles. Note that in these "live" simulations, however, the disks are not self-gravitating, so that instabilities cannot develop.

I simulate an extensive simulation of $N = 10^4$ equal mass (*i.e.*: no mass spectrum) planetesimals for planet in a fixed initial position (22 A.U.) embedded in a planetesimal disk with a size of 8 A.U. For the simulations proposed here I use a numerical integrator called SyMBA ([27] and references therein). To speed up the simulations I used an OPEN-MP version of SyMBA written by D. Minton. Here the number of planetesimals is small due to the fact that I am not interested in simulating a self-gravity massive

planetesimal disk. First, I start the simulations with planetesimals distributed in a ring of 1 A.U. in size and a planet in an outer or inner orbits with respect to the annulus to study the dependence of the position and planet mass on the torque. After these first simulations, I start to follow the planet migration for a considerable part of the disk so I must concentrate on an extended region of planetesimals disk. Furthermore, since the accretion and migration processes time scales can be often comparable and because I do not want to reproduce *accretional migration* but only gravitational interaction and angular-momentum exchange. I reduce the collisional radius of the planet one order of magnitude smaller than radius of the Earth (for every simulations) and put the Hill radius and the collisional radius of the planetesimals equal to zero to avoid close encounter between planetesimals themselves. It is impossible to reduce further the planet radius due to the integration time (the code reduces the timestep each time a close encounter is realized). Anyway a good method to monitor the accretional processes is the study of the eccentricity variation Δe during all the simulation; this parameter in fact is correlated with mass accretion ΔM as follows [28]:

$$\Delta e = \frac{\Delta M}{M_P}\,, \tag{2}$$

where M_P is the planet mass at the beginning of the simulation.

2˙3. *Mock observations.* – Finally I simulate the emission at a specific wavelength from the disk and observe it with ALMA.

The results of the simulations where processed by using the software CASA (the Common Astronomy Software Applications package). This software allows to simulate disks as observed with ALMA (Atacama Large Millimeter Array). The ALMA interferometer is an array of 66 antennas (ranging from 7 to 12 m) which observe a particular region of the sky in the mm to sub-mm range (from 380 μm to 3.6 mm). For ALMA, in the configuration with the longest baseline, the resolutions ϕ is equal to $0.001''$ (arcsec) in the mm range([2]). This allows to observe object as the protoplanetary disk at distances greater than 100 pc. For a planetesimal disk the need of sub-mm observation is due to the absence of gas emissions. In fact, the major emission comes from the grains. In [18] they describe the presence of cavities in the protostellar disk in which the brightness profile is lower with respect to the rest of the disk. For the simulations I use a flux of 10 mJy at 900 GHz (which permits the highest resolution for ALMA, fixing the baselines configuration). This flux is similar to the one of Fomalhaut [29]. I simulate a disk with different size and inclination with the planet in different position, masses and orbit ("prograde" or "retrograde"). I follow some of Wolf prescriptions for the disks [30]. The host star has a mass equal to the mass of the Sun ($M_* = 1M_\odot$), and the disk has a lower mass, for a planet with the mass of the Earth, equal to $M_{disk}^{low} = 5 \times 10^{-4} M_\odot$ and, for a planet with the mass of Jupiter, equal to $M_{disk}^{up} = 2.5 \times 10^{-2} M_\odot$ (similar to [31]). The bandwidth of the observation is equal to 8 GHz.

([2]) The resolution of an interferometer can be calculated from the *synthesized beam* $\phi = 1.22\frac{\lambda}{D}$ which depends on the distance between antennas D (*baseline*) and on the wavelength of the observation (λ).

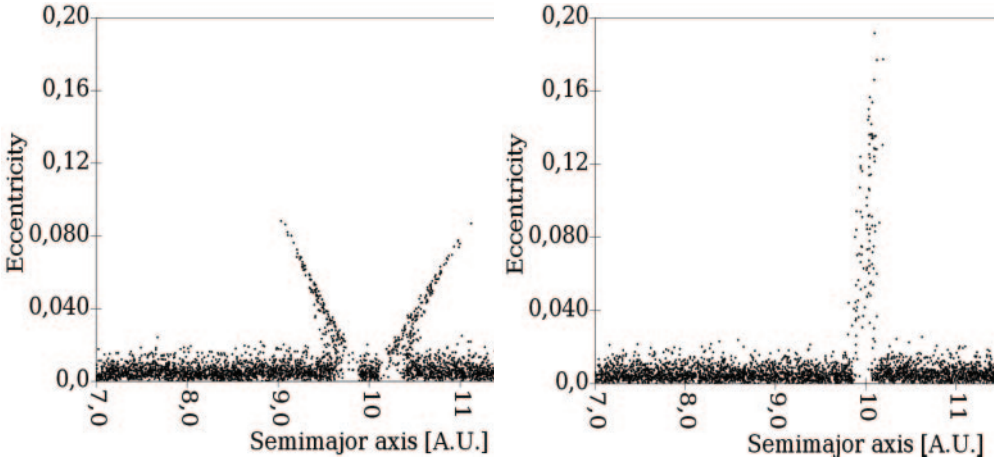

Fig. 1. – The a-e plane for both a prograde and a retrograde planet of mass equal to $1M_\oplus$. The prograde case (a) present the normal double Jacobi wing with respect to the counter-rotating planet (b) which presents a particular single Jacobi wing feature.

3. – Results

I now summarize the results of the numerical simulations. Only a part of the numerical simulations are reproduced in this preliminar work due to their large number.

3˙1. *Dead planet.* – In fig. 1 is shown a simulation for a $1\,M_\oplus$ planet in the co- and counter-rotating orbits. Is it possible to see how the different inclination of the planet changes the disk in different ways. The retrograde planet, due to the absence of resonances [15] creates different "Jacobi wings" (planetesimals in the semimajor axis-eccentricity plane with particular combination of e and a due to the conservation of Jacobi integral [8]) and no resonance overlap regions so the gap in this simulation is smaller than in the prograde case and is equal to the gravitational section of the planet with a half size equal to 1 R_H. For the prograde case, instead, the resonances overlap near the planet and create a larger gap with half size equal to 3.5 R_H [32, 33].

In the figure the presence of resonances is not clear due to the initial Rayleigh distribution of planetesimals that cover the increasing in planetesimals eccentricity in the resonance regions. A useful formula for calculating the gap width is [34]

$$\Delta a = a_P \left[\frac{4}{3} \left(e_P^2 + i_P^2 \right) + 12 \left(\frac{r_H}{a_P} \right)^2 \right]^{1/2}_{e_P, i_P = 0} \simeq 7 r_H, \tag{3}$$

where r_H is the Hill radius of the object ($r_H \simeq a_P (M_P/M_*)^{1/3}$), a_P the semimajor axis of the planet and e_P and i_P are, respectively, the eccentricity and the inclination of the planet.

3˙2. *Live planet.* – The analytical theories [5] and [35] predict that the migration rate for a counter-rotating disk of planetesimal is higher with respect to the co-rotating case. Figure 2 shows four simulations of a planet with mass of $10M_\oplus$, a semimajor axis of 22 A.U., and a planet-to-planetesimal mass ratio equal to 1/600 (for the initial conditions of

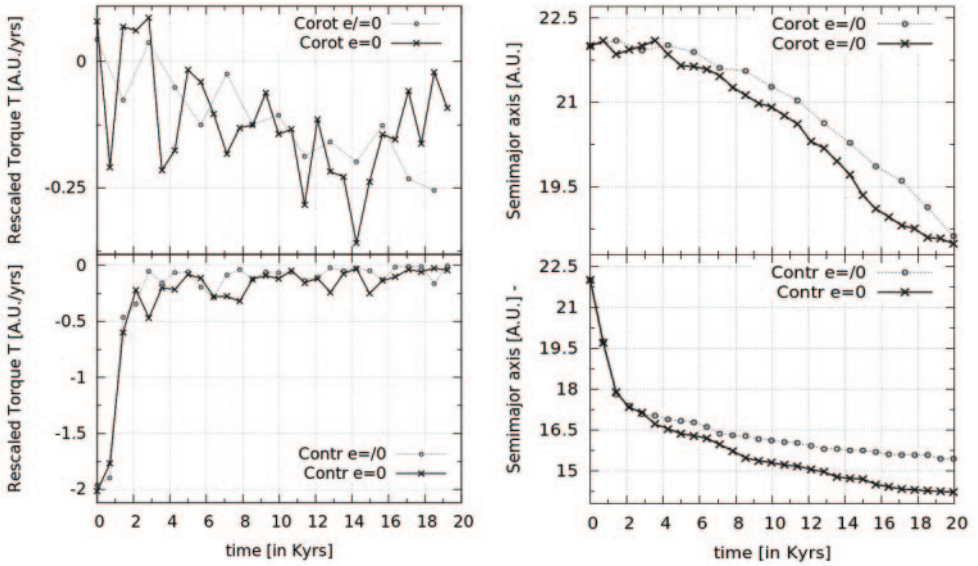

Fig. 2. – Right panel: planet migration rate for a co- and a counter-rotating planet embedded in a planetesimal disk. The counter-rotating planet (dashed-circle line) migrates faster than in the prograde case (dashed-cross line). Left panel: torque of the planet *versus* time. The rescaled torque (multiplied by 0.5×10^6) is clearly different in the two cases.

the planetesimal disk see sect. **2**). Each simulation describes a particular initial condition for the planet: "prograde" or "retrograde" case and with ($e = /0$) or without ($e = 0$) an eccentricity distribution for planetesimals.

To analyze the different migration rate of the planet in the counter- and co-rotating case I perform the study of the angular-momentum variation in time and the torque exerted on the planet by the planetesimals. Here I introduce only the values taken from the simulations, in the following section I discuss and compare these results with the ones obtained from the analytical theories. The angular momentum of a planet in an eccentric orbit (e) with mass M_P and with a semimajor axis a_P is equal to

$$L_P = M_P \sqrt{G M_* a_P (1 - e^2)}, \tag{4}$$

where M_* is the mass of the central star. The rate of the angular momentum exchanged by the planet is also equal to the torque Γ exerted by the disk to the planet divided by the angular momentum of the planet and can be obtained from the migration rate of the planet, as follows:

$$\frac{\dot{L}_P}{L_P} = \frac{1}{2}\frac{\dot{a}_P}{a_P} - \frac{e_P^2}{1 - e_P^2}\frac{\dot{e}_P}{e_P}\frac{\Gamma}{L_P}\,. \tag{5}$$

The migration rate, fixing all the other parameters: planet mass, planetesimal mass, density distribution and extension of the disk and position of the planet, depends on the inclination of the planet and on the eccentricity distribution of plantesimals. From fig. 2

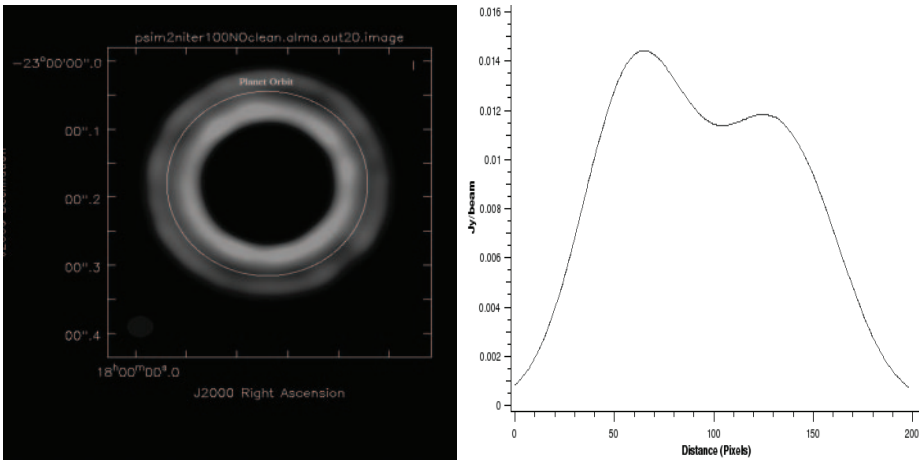

Fig. 3. – Left panel: Mock observation of a retrograde planet (10 $M_\oplus$). The planet mass is equal to $10M_\oplus$ for each simulations. The disk is 100 A.U. in size and at a distance of 100 pc. Right panel: Surface brightness profile of the disk. It is possible to observe a gap that is larger with respect to the one created by a prograde migrating planet due to the different migration rate. The absence of the 1 : 1 resonance region is due to the absence of the mean motion resonance in this counter-rotating case.

is it possible to observe that the retrograde torque is more negative but also tends to zero more quickly with respect to the prograde case.

3˙3. *Observational features.* – A lot of study as been done for the SED (Spectral Emission Distribution) of a protoplanetary disk [36] and it has been shown that a cavity, or a baroclinic vortex, modify substantially the emission of a protostellar disk ([30] and references therein). Conversely of the radial velocity detection method, the efficiency of the gap detection method using direct imaging increases with the distance of the planet: A more distant planet possesses a larger feeding zone (or cavity). For every single image is it possible, using the brightness profile, to calculate the gap size and using that to estimate the mass of the planet (fig. 3).

4. – Discussion and conclusions

In this paper I have studied the migration of a planet in a plantesimal disk with both numerical simulations and analytical theories. I perform different sets of numerical simulations of a retrograde and a prograde planet embedded in disks with or without a Rayleigh distribution in eccentricity for planetesimals. For all the simulations I use different initial mass for the planet (1, 10, 100 and 300 $M_\oplus$).

I found, as not yet shown in the literature, that the migration rate for the co-rotating case is sensible to the eccentricity distribution of planetesimals: the higher the eccentricity the higher the migration rate.

A new trend that I found from simulations is that the counter-rotating disk has a higher migration rate than the co-rotating case. Another new result for the "retrograde" case is that the migration rate of the planet is not dependent on the eccentricity distribution of the planetesimal disk. This can be understand noting that in this case the

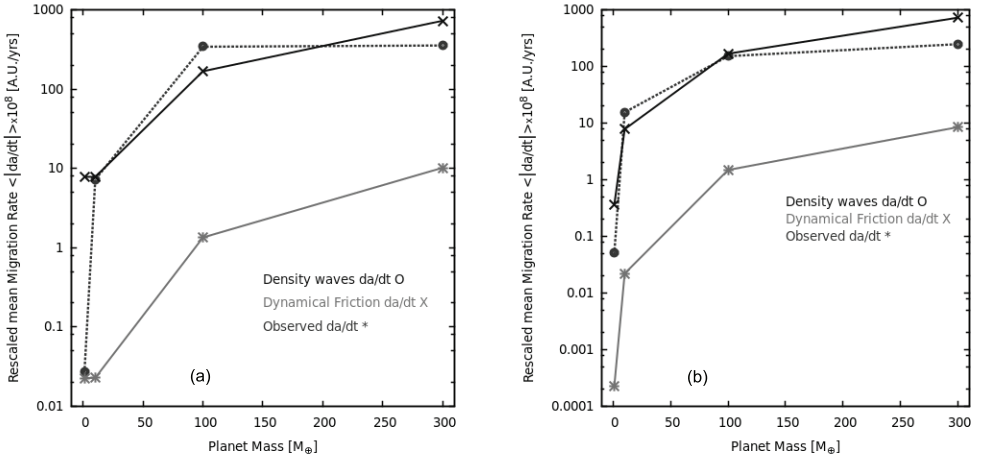

(a) (b)

Fig. 4. – In this figure the torque for four planets of different mass (1, 10, 100 and 300 $M_\odot$) is shown for both the co- and counter-rotating cases (a, b, respectively). The mean value of the torque (dashed line red circle) is calculated from the simulation while for the dynamical friction torque I use [37] (continuous line green asterix) and [35] for the linear theory of density waves (continuous line blue cross). (a) Mean migration rate of retrograde planets with an inner ring of planetesimals. (b) Mean migration rate of prograde planets with an inner ring of planetesimals.

very important physical mechanism that drives the angular-momentum exchange and the migration is the relative angular frequency difference between planet and planetesimals. For the retrograde case this creates a very high exchange of angular momentum between planet and disk that generates a *fast planet migration* model. I found also that the migration rate is linear dependent on planet mass as in the dynamical friction case: the more massive the planet the higher the migration rate. This is true for both the "prograde" and "retrograde" cases. This features is confirmed also with the linear theory of density waves. In fig. 4 the calculation of the rescaled mean torque $\langle\Gamma\rangle$ is shown both from the numerical simulations and with the linear theory of density waves [35] and dynamical friction [37] for a planet in prograde and retrograde orbit with an inner ring of planetesimals.

Observing the mean migration rate comparison, the linear theory of density waves match well with the numerical simulations respect to the dynamical friction. This because the dynamical friction formula introduced here does not use a velocity distribution and so the theory gives only a first-order approximation of the simulated data.

The simulations confirm also the direct dependence on the density of planetesimals: the larger the density the higher the migration rate both in the "prograde" that in the "retrograde" cases. I found also a change in the signs of the migration rate (from inward to outward migration) between simulations of the same planetesimals rings but with a different mass for the planet, keeping the distance between planet and planetesimal ring to be constant, this is due to the definition of *close encounter*: when the planetesimals are "near" the planet every encounter generate a semimajor axis variation which carries the planet closer to the disk [38]. The definition of "near", however, is dependent on the Hill Radius and so it is directly dependent on the mass of the planet: the higher the mass of the planet, fixing its semimajor axis, the larger the *close encounter* zone.

When the planet is embedded in a planetesimal disk that is very extensive with respect to the feeling zone, the contribution of resonances far from the planet (and then, far from the *close encounter* zone) modifies the migration rate and also the direction of the migration. In fact the *distant encounter* migration rate is always repulsive and generates two opposite torques from the inner and the outer part of the disk to the planet, the net torque exchanged is always positive and in this case only the inward migration can be found in the simulations. Finally the study of the planetesimals disk with ALMA allows to detect not only the presence of a planet that is, otherwise, not so luminous to be observed but also the mass and its inclination from the properties of the disk in which it is embedded, in particular: the gap extension is related with the mass of the planet and the presence or absence of $1:1$ mean the motion resonance allows to distinguish between the counter-rotating and the co-rotating case.

* * *

I thank Stefano Meschiari for very helpful comments and suggestions on this work. I also thank M. Massardi for very helpful corrections on my Master Thesis. Finally I am also grateful to D. Kaufmann, for his unwavering patience that he showed answering several technical questions.

REFERENCES

[1] Mayor M. and Queloz D., *Nature*, **378** (1995) 355.
[2] Howard A. W., *Science*, **340** (2013) 572.
[3] O'Brien D. P., Morbidelli A. and Levison H. F., *ICARUS*, **184** (2006) 39.
[4] Ida S. and Makino J., *Astrophys. J.*, **403** (1992) 336.
[5] Del Popolo A., Gambera M. and Ercan N., *Mon. Not. R. Astron. Soc.*, **325** (2001) 1410.
[6] Fernandez J. A. and Ip W. H., *ICARUS*, **58** (1984) 109.
[7] Walsh K. J. and Morbidelli A., *Astron. Astrophys.*, **526** (2011) 8.
[8] Kirsh D. R., Duncan M., Brasser R. and Levison H. F., *ICARUS*, **199** (2009) 197.
[9] Bromley B. C. and Kenyon S. J., *Astrophys. J.*, **764** (2013) 19.
[10] Bromley B. C. and Kenyon S. J., *Astrophys. J.*, **735** (2011) 15.
[11] Crida A., Papaloizou J. C. B., Rein H., Charnoz S. and Salmon J., *Astron. J.*, **140** (2010) 944.
[12] Roedig C. and Sesana A., *Mon. Not. R. Astron. Soc.*, **439** (2013) 3476.
[13] Kozai Y., *Astron. J.*, **67** (1962) 591.
[14] Teyssandier J., Naoz S., Lizarraga I. and Rasio F. A., *Astrophys. J.*, **779** (2013) 14.
[15] Morais M. H. M. and Namouni F., *Cel. Mech. Dyn. Astron.*, **117** (2013) 405.
[16] Hillenbrand L. A., Hoffer A. S. and Herczeg G. J., *Astron. J.*, **146** (2013) 16.
[17] Bate M. R., Lubow S. H., Ogilvie G. I. and Miller K. A., *Mon. Not. R. Astron. Soc.*, **341** (2003) 213.
[18] Ozernoy L. M., Gorkavyi N. N., Mather J. C. and Taidakova T. A., *Astrophys. J.*, **537** (2001) L147.
[19] Semenov D., Pavlyuchenkov Y., Henning T., Wolf S. and Launhardt R., *Astrophys. J.*, **673** (2008) L195.
[20] Jang-Condell H., *Astrophys. J.*, **700** (2009) 320.
[21] Lagrange A.-M. *et al.*, *Science*, **329** (2010) 57.
[22] Telesco C. M. *et al.*, *Nature*, **433** (2005) 133.
[23] van der Marel N. *et al.*, *Science*, **340** (2013) 1199.
[24] Hahn J. M. and Malhotra R., *Astron. J.*, **117** (1999) 3041.
[25] `http://www.boulder.swri.edu/swifter`.

[26] Levison H. F. and Duncan M. J., *ICARUS*, **108** (1994) 18.
[27] Levison H. F. and Duncan M. J., *Astron. J.*, **120** (2000) 2117.
[28] Nixon C. J., Cossins P. J., King A. R. and Pringle J. E., *Mon. Not. R. Astron. Soc.*, **412** (2010) 1591.
[29] Walsh J. and Testi L., *The Messenger*, **148** (2012) 32.
[30] Wolf S., *Adv. Space Res.*, **40** (2007) 625.
[31] Gonzalez J. F., Pinte C., Maddison S. T., Ménard F. and Fouchet L., *Astron. Astrophys.*, **547** (2012) 15.
[32] Murray C. D. and Dermott S. F., *Solar System Dynamics* (Cambridge University Press) 2001.
[33] Morbidelli A., *Modern Celestial Mechanics, Aspects of Solar System Dynamics* (Taylor and Francis, London) 2002.
[34] Wetherill G. W. and Stewart G. R., *ICARUS*, **106** (1993) 190.
[35] Cionco R. G. and Brunini A., *Mon. Not. R. Astron. Soc.*, **334** (2002) 77.
[36] Bruderer S., van der Marel N., van Dishoeck E. F. and van Kempen T. A., *Gas structure inside dust cavities of transition disks: Oph IRS* 48 *observed by ALMA*, arXiv:1312.2756 [astro-ph.SR] (2013).
[37] Lin D. N. C. and Papaloizou J., *Mon. Not. R. Astron. Soc.*, **188** (1979) 191.
[38] Ormel C. W., Ida S. and Tanaka H., *Astrophys. J.*, **758** (2012) 17.